Published in final edited form as:
Neuroimage. 2006 December ; 33(4): 1029–1035.

Pattern of Hemodynamic Impairment in Multiple Sclerosis: Dynamic Susceptibility Contrast Perfusion MR Imaging at 3.0 T

Sumita Adhya, MS, **Glyn Johnson, PhD**, **Joseph Herbert, MD***, **Hina Jaggi, MS**, **James S. Babb, PhD**, **Robert I. Grossman, MD**, and **Matilde Inglese, MD, PhD**
*Department of Radiology, and *Department of Neurology, Hospital for Joint Disease New York University School of Medicine, 650 First Avenue, New York, NY 10016, USA*

Abstract

This study aimed to determine regional pattern of tissue perfusion in the normal-appearing white matter (NAWM) of patients with primary-progressive (PP), relapsing-remitting (RR) multiple sclerosis (MS) and healthy controls, and to investigate the association between perfusion abnormalities and clinical disability. Using dynamic susceptibility contrast (DSC) perfusion MRI at 3 Tesla, we studied twenty-two patients with clinically definite MS, eleven with PP-MS and eleven with RR-MS and eleven age- and gender-matched healthy volunteers. The MRI protocol included axial dual-echo, dynamic susceptibility contrast enhanced (DSC) T2*-weighted and post-contrast T1-weighted images. Absolute cerebral blood flow (CBF), cerebral blood volume (CBV) and mean transit time (MTT) were measured in the periventricular, frontal, occipital NAWM, and in the splenium of the corpus callosum. Compared to controls, CBF and CBV were significantly lower in all NAWM regions in both PP-MS patients (p values from <0.0001 to 0.001) and RR-MS (p values from <0.0001 to 0.020). Compared to RR-MS, PP-MS patients showed significantly lower CBF in the periventricular NAWM (p= 0.002) and lower CBV in the periventricular and frontal NAWM (p values: 0.0029 and 0.022). EDSS was significantly correlated with the periventricular CBF (r=−0.48, p=0.0016) and with the periventricular and frontal CBV (r=−0.42, p=0.015; r=−0.35, p=0.038, respectively). This study suggests that the hemodynamic abnormalities of NAWM have clinical relevance in patients with MS. DSC perfusion MRI might provide a relevant objective measure of disease activity and treatment efficacy.

Introduction

Multiple Sclerosis (MS) has traditionally been viewed as a chronic inflammatory/ demyelinating disease of the central nervous system (CNS) (Hauser, 1994). Axonal damage, although acknowledged in the earliest description of the disease (Hauser, 1994), has been recognized as the prominent pathological substrate of irreversible disability only in the past few years (Trapp et al., 1999). Axonal injury is not restricted to macroscopic lesions (Trapp et al., 1998) but extends into the normal appearing white matter (NAWM) which is affected at varying degrees of severity and extent (Evangelou et al., 2000). However, the timing and the nature of molecular mechanisms leading to neurodegeneration as well as those that prevent regeneration in MS are still a matter of active investigation and are likely to be multifactorial.

Cerebral perfusion has been shown to be reduced not only in stroke (Latchaw, 2004) but also in several degenerative diseases of the CNS such as Alzheimer's and Parkinson's diseases, epilepsy, HIV-cognitive motor complex and MS (Chang et al., 2000; Firbank et al., 2003;

Address communications and reprints request to: Matilde Inglese, MD, PhD, Department of Radiology, New York University School of Medicine, 650 First Avenue, 6th floor, New York, NY 10016, Tel./FAX (212) 263-3322; (212) 263-7542, e-mail: matilde.inglese@med.nyu.edu.

Johnson et al., 2005; Rashid et al., 2004; Warach et al., 1994). It is therefore possible that perfusion abnormalities contribute to neuroaxonal degeneration and one may speculate that reduced blood supply leads to a higher probability of permanent tissue destruction.

Very little is known about perfusion changes in the NAWM of patients with MS. Early studies with dynamic susceptibility contrast-enhanced (DSC) perfusion MRI (pMRI) focused on lesions and measured relative perfusion values expressed as a ratio to the perfusion of contralateral NAWM (Haselhorst et al., 2000; Wuerfel et al., 2004). However, NAWM is, in reality, abnormal in MS, and so makes an inappropriate reference. A more recent study employing absolute measures of flow and volume has reported decreased cerebral blood flow (CBF) in the NAWM of patients with relapsing-remitting (RR) MS (Law et al., 2004). Conversely, elevation of CBF and cerebral blood volume (CBV) has been reported in NAWM of RR-MS patients several weeks before focal leakage of the blood brain barrier (BBB) and plaque formation. Both these studies suggest that bolus tracking perfusion might provide a sensitive measurement of disease activity and treatment effect (Wuerfel et al., 2004).

In approximately 10–15% of cases, MS follows a primary progressive (PP) course characterized by a progressive clinical decline without superimposed exacerbations (Noseworthy, 1999). Compared to patients with the most common RR course of the disease, PP-MS patients are older and have fewer lesions on MRI scans. In addition, the rate of new lesion formation is lower and gadolinium-enhancing lesions, an indicator of BBB breakdown associated with inflammation, are relatively rare (Thompson et al., 1991). The smaller degree of inflammation, as well as the lower sensitivity of the classical MRI outcome measures, may explain the negative results of treatment trials with antinflammatory agents in PP-MS (Leary and Thompson, 2003; Wolinsky, 2006). The question remains as to the nature of the non-inflammatory mechanism of disability that is operating in the majority of PP-MS patients who do not show enhancement.

The purpose of this study was three-fold: *a)* to determine regional patterns of hemodynamic changes in the NAWM of PP-MS and RR-MS patients by utilizing DSC pMRI at 3 Tesla; *b)* to compare the NAWM perfusion pattern of RR-MS, where inflammation and demyelination are predominant, with that of PP-MS whose prominent pathological feature is neurodegeneration; *c)* to assess the impact of perfusion abnormalities on neurological deficits

Materials and Methods

Subjects

Eleven (3 male and 8 female) consecutive patients with RR-MS and 11 (7 male and 4 female) consecutive patients with PP-MS meeting the McDonald criteria (McDonald et al., 2001) were prospectively enrolled in the study. Neurologic disability was assessed by a single experienced neurologist (J. H.) blind to the MRI findings using the Expanded disability status scale (EDSS) score (Kurtzke, 1983) within 1 week of MRI. Patients were not included if they had corticosteroid use or relapses within 3 months prior to MRI. The patient with PP-MS had a mean age of 53.63 (range, 29–71) yrs, median disease duration of 4 (range, 1–19) yrs and median EDSS score of 4 (range, 3–7). The patients with RR-MS had a mean age of 46.18 (range, 31–71) yrs, median disease duration of 5 (range, 1–13) yrs and median EDSS score of 1.0 (range, 0–6.5). Only RR-MS patients were under immunomodulatory treatment with Interferon beta-1a (Avonex, Biogen, Cambridge Mass), Interferon beta-1a (Rebif, Serono, Rockland, MA) and glatiramer acetate (Copaxone, Teva, Petah Tiqvah, Israel). For comparison, eleven age- and gender-matched healthy controls (4 male and 7 female) were recruted. Their mean age was 50.82 (range, 29–65) yrs. Approval for this study was obtained from the Institutional Board of Research Associates of New York University Medical Center

and informed consent was obtained from all subjects. Demographic and clinical charachteristics of the three subject groups are given in Table 1

MR Imaging Acquisition

MRI was performed using a 3.0-T scanner (Trio, Siemens Medical Systems, Erlangen, Germany) with an 8-channel phased-array head coil. The following sequences were collected in all subjects during a single MR session: *a)* dual-echo turbo spin-echo (repetition time [TR] = 5,500, echo time [TE] = 12/99, 96 contiguous, 3 mm-thick, axial slices with a 256 x 205 matrix and a 220 x 190 mm field of view [FOV]; in-plane voxel-size 1.1 x 0.9; parallel imaging acceleration factor of 2); *b)* gradient-echo echo-planar imaging (TR = 1000, TE = 32; 10 contiguous, 3 mm-thick axial slices with a 128 × 128 matrix; 220 × 220 FOV; flip angle, 30°; and signal bandwidth, 1396 Hz/pixel; in-plane voxel size, 1.7 × 1.7 mm). DSC MR images were acquired during the first pass of a standard-dose (0.1 mmol/kg) bolus of gadopentetate dimeglumine (Magnevist; Berlex Laboratories, Wayne, NJ). Contrast was injected at a rate of 5 mL/sec, followed by a 20-mL bolus of saline also at a rate of 5 mL/sec. A total of 60 images were acquired at 1-second intervals, with the injection occurring at the fifth image, so that the bolus would typically arrive at the 15th to 20th image. *c)* Post-Gd T1-weighted spin-echo (TR = 471, TE = 12, 50 contiguous, 3 mm-thick, axial slices with a 256 x 205 matrix and a 220 x 220 mm FOV, in-plane voxel size 1.1 x 0.9).

Image Processing and Evaluation

Data were transferred to a Linux workstation for offline perfusion analysis using programs developed in-house using the IDL programming languages. In all cases contrast agent concentration, C, is first found using the simple relationship (Rosen et al., 1991)

$$C \propto -\ln\left(\frac{S}{S_0}\right)$$

where S is the signal intensity and S_0 is the pre-bolus signal intensity. This equation assumes that T1 shortening effects are negligible which is true in practice since we use a relatively low flip angle to minimize saturation.

Absolute cerebral blood volume (CBV), cerebral blood flow (CBF) [*cf.*, figure 1] and mean transit time (MTT) were calculated using the method of Rempp *et al*. (Rempp et al., 1994). These parameters can be calculated from the following equations:

$$MTT = \frac{\int C dt}{C_{max}}$$

$$CBV = \frac{\int C dt}{\int AIF dt}$$

$$CBF = \frac{CBV}{MTT}$$

where C is the tissue concentration following an ideal, instantaneous bolus and C_{max} is the maximum value of C. The bolus is not instantaneous, of course, but an approximation to the idealized response can be found by deconvolving the measured tissue concentration with the arterial input function (AIF). The AIF was found using an automated method similar to that described by Rempp *et al.* (Rempp et al., 1994) and Carroll *et al*. (Carroll et al., 2003).

MTT, CBV, and CBF were calculated in regions of interest (ROIs) in four brain locations: periventricular, frontal, occipital NAWM, and the splenium of the corpus callosum (CC). To optimize reproducibility, CBF, CBV, and MTT measurements were taken in two ROIs in each of the four locations. ROIs were fixed in size (radius 1 image pixel, 1.8 mm) and were placed to avoid arterial and venous structures in the NAWM, particularly in the subcortical and periventricular areas. ROIs were placed in the same section positions in patients and controls. Within these section positions, ROIs were placed in the same locations within the four brain regions described above. Perfusion measurements were obtained by two authors with more than five years of experience with this type of measurement in clinical and research settings and blinded to patients' identity. To exclude inter-observer and minimize intra-observer variability as to the location of ROI placement between patients, each patient data set was reviewed by both authors at the same time (Wetzel et al., 2002). Furthermore, the ROIs were placed after visual co-registration with the transverse T2-weighted images to ensure that lesions were not included in the ROIs.

Intraobserver reproducibility of DSC-MRI measures of the NAWM was also assessed. On two separate occasions (separated by at least 3 months), the same observer measured CBF, CBV and MTT of the above-mentioned NAWM areas from 6 healthy controls. The mean intraobserver coefficients of variation for CBF, CBV and MTT were lower than 24% for all the NAWM regions studied.

Lesion Volume Measurements

T2-hyperintense and T1-hypointense lesion volume (LV) measurements were performed by a single trained technician, blinded to subject identity, using a semiautomated segmentation technique based on local thresholding (Jim version 3, Xinapse Systems, UK, http://www.xinapse.com), using the marked hardcopies as a reference (Bermel et al., 2003). Out of 22 patients only one affected by RR-MS presented 2 gadolinium-enhancing lesion on post-contrast T1 scans.

Statistical Analysis

Mixed model analysis of variance was used to evaluate differences among subject groups in terms of each perfusion measure while adjusting for the potential confounding effects of age and gender. A separate analysis was conducted for each perfusion measure. In each case, the values observed in the left and right sides of each brain region of every subject constituted the dependent variable. The model included patient age and gender as covariates, side, region and subject group as fixed classification factors as well as the term representing the interaction between brain region and subject group (the interaction tests whether differences among groups are stable across brain regions). The covariance structure was modeled by assuming observations to be correlated or independent when derived for the same subject or different subjects, respectively, with the strength of correlation dependent on whether or not the observations came from the same brain region, and by allowing the error variance to differ across subject groups and brain regions.

Within the mixed model format, Tukey's honest significantly different (HSD) procedure was used to make all pairwise comparisons among subject groups with respect to each perfusion measure within each brain region while adjusting for age and gender and maintaining the familywise type I error rate for the set of comparisons at or below the 5% level. In MS patients, the mixed model analysis was also used to examine the association of each perfusion measure with EDSS, T2, T1 lesion volume and disease duration. The analysis followed the same outlined as described above excepting only that the model now included either disease duration, lesion volumes or EDSS as well as terms representing the interactions of the included measure of disease severity or duration with subject group and brain region. All reported p values are

two-sided and HSD-adjusted and were declared statistically significant at the 5% level. All statistical computations were carried out using SAS for Windows version 9.0 (SAS Institute, Cary, NC, 2002).

Results

None of the healthy controls showed lesions on T2- and T1-weighted scans. T2 and T1 LV for the MS patients are given in Table 1.

There were no significant differences among the three groups of subjects in terms of MTT ($p>0.3$ for all comparisons). Results pertaining to group comparisons with respect to CBF and CBV are given in Table 2 and Figure 2.

Comparison of Perfusion metrics between Patients with PP-MS, RR-MS and Controls

After adjustment for age and sex, significant differences were found between the PP-MS patients and the controls with respect to the CBF ($p<0.0001$) and CBV ($p<0.001$) in all four regions of NAWM. Also, significant differences were found between the RR-MS patients and controls with respect to CBF ($p<0.0006$) in all four regions of NAWM. With respect to the CBV, there were significant differences in periventricular, frontal, and occipital NAWM ($p<0.02$) but not in the splenium ($p=0.08$). Finally, significant differences were found between the patients with PP-MS and RR-MS with respect to CBF in the periventricular NAWM ($p=0.002$) but not in frontal, occipital and splenium ($p>0.085$). With respect to CBV, there were significant differences in periventricular and frontal NAWM ($p=0.029$ and 0.022, respectively) but not in the occipital NAWM and splenium ($p=0.97$ and 0.25).

Correlations between Perfusion metrics, lesion volumes, disease duration and EDSS

Neither T2 and T1 LVs, nor disease duration correlated with the perfusion metrics from the four regions of NAWM. The EDSS score was significantly correlated with the periventricular NAWM CBF value ($r = 0.48$, $p=0.0016$) and with the periventricular and frontal NAWM CBV value ($r = 0.42$, $p=0.015$; $r = 0.35$, $p=0.038$). There was no significant correlation between MTT and disease duration, EDSS score or either measure of lesion volume.

Discussion

Although conventional MRI (cMRI) is valuable in detecting white matter plaques associated with MS, it lacks pathological specificity and sensitivity to functional and microstructural abnormalities affecting NAWM (Miller et al., 2003). In PP-MS, cMRI is less useful in monitoring disease activity and response to treatments due to the lower lesion formation rate and level of gadolinium enhancement (Thompson et al., 1991).

DSC perfusion MR may partially overcome the limitations of conventional MRI by characterizing cerebral microvascular hemodynamics. In addition, DSC perfusion MRI performed at 3 T field strength provides several advantages relative to that performed at 1.5 T. Intrinsic signal-to-noise ratio is higher. Sensitivity to T2* changes due to contrast agent is increased. This can be traded off for either lower contrast dose or, a shorter TE and hence a larger number of slices and improved coverage within a fixed TR. Although distortion and blurring due to susceptibility effects are also increased, this can be offset, at least partially, by the use of shorter TEs (Manka et al., 2005).

Our study demonstrates that, compared to healthy controls, both patients with RR-MS and with PP-MS show widespread reduced CBF and CBV in the NAWM. Although CBF and CBV values were generally lower in PP-MS than in RR-MS, the difference reached statistical significance only in the periventricular and frontal NAWM. In general, the finding of regional

NAWM hypoperfusion is in agreement with the results derived from nuclear medicine studies of cerebral perfusion in MS (Brooks et al., 1984; Lycke et al., 1993; Pozzilli et al., 1991) and with two previous MRI studies (Law et al., 2004; Rashid et al., 2004). Using DSC MRI, Law *et al*. reported a significant decrease of CBF and a prolongation of MTT in the NAWM at the level of lateral ventricles in RR-MS patients (Law et al., 2004). In our study, NAWM perfusion was measured not only at the level of lateral ventricles but also at the level of frontal and occipital NAWM and in the splenium of the corpus callosum. The difference between these two studies might be due to differences in disease duration and severity of disability of patients' groups. Similarly, Rashid *et al*. using arterial spin labeling observed decreased NAWM perfusion especially adjacent to areas of decreased deep gray matter in patients with progressive MS. Interestingly, they observed small foci of increased perfusion only in the NAWM of RR-MS patients not being treated with any immunomodulatory drugs (Rashid et al., 2004).

Taken together these findings seem to suggest that microvascular impairment may play a role in the pathogenesis of MS. It is well known that inflammation may result in microvascular damage by different mechanisms. Cytotoxic T cells may recognize their antigen directly on the luminal surface of brain vessels. The subsequent apoptosis of endothelial cells may activate a clotting cascade leading to thrombosis. Likewise, specific antibodies may recognize their antigen at the vessel wall and induce endothelial and vascular damage by complement activation or through macrophage toxins. Endothelial cells can also be damaged directly by pro-inflammatory cytokines. Furthermore, edema associated with inflammation leads to focal tissue swelling which may result in a disturbance of microcirculation (Lassmann, 2003). Indeed, microvascular involvement in MS has been reported by both histological and MRI studies (Haselhorst et al., 2000; Law et al., 2004; Putnam, 1933; Putnam, 1935; Rashid et al., 2004; Wakefield et al., 1994). The disease involves an inflammatory response with BBB destruction, exudation of inflammatory cells as well as vasculitis of the small veins (Adams et al., 1985). Acute and chronic venous obliterations have been described as well as perivascular and intravascular fibrin deposition (Adams et al., 2004). Intuitively, in addition to direct vascular endothelium injury, obliterative vasculitis might result in chronic ischemia and diffuse parenchymal damage through the modulation of vascular tone and CBF.

Although the lower level of MRI-visible inflammation in PP-MS is supported by reduced cellularity and number of perivascular cuffs seen histologically (Bruck et al., 2002), it has been suggested that the inflammation may be less severe but persists for a longer time when compared to RR-MS. Patients with PP-MS have a higher proportion of bcl-2-expressing T cells in their lesions, suggesting an impaired elimination of inflammatory cells (Zettl et al., 1998). More recently, Ingle *et al*. have shown that enhancement is present in some cases of early PP-MS and is associated with greater disease impact. Thus the presence of an inflammatory process in a preclinical phase cannot be excluded (Ingle et al., 2005).

It is known that NAWM abnormalities depend only in part on the degeneration of fibers passing through discrete white matter lesions (Loevner et al., 1995; Rovaris et al., 2005b). Microscopic lesions, beyond the resolution of conventional MRI are also believed to contribute to NAWM abnormalities. In our study, neither T2 nor T1 lesion loads correlated with NAWM CBF and CBV values in both patient groups. This is not surprising for the PP-MS group, where the occult and diffuse pathology in normal-appearing tissue can occur independently of the presence of MRI visible lesions (Rovaris et al., 2005a). Admittedly, since lesion volume was assessed on the whole brain whereas the perfusion measures were collected on a regional basis, the lack of correlation might be due to technical limitations. Future studies assessing the global NAWM perfusion abnormalities using histogram analysis should help clarify this point. Although it would have been of great interest, it was not possible to investigate the relationship between inflammation as indicated by gadolinium-enhancement and hemodynamic impairment since only one RR-MS patient showed gadolinium-enhancement (Rudick, 1999).

An important finding of this study was the correlation between regional hemodynamic impairment in the periventricular and in the frontal regions and the clinical disability. This provides further evidence that tissue changes undetectable on conventional scanning may be functionally relevant. However, EDSS measurements are weighted towards locomotor disability, which is likely to depend on the amount of spinal cord damage (Kurtzke, 1983). Future studies employing cognitive measures may demonstrate a better correlation with the hemodynamic dysfunction.

This study is not without limitations. Our subgroups of patients were small and did not show gadolinium-enhancement precluding us from investigating the relationship between inflammation and changes in tissue perfusion. Furthermore, the DSC MRI algorithm is based on the assumption of negligible dispersion in the bolus between the arteries where the AIF is measured and the tissue of interest. To minimize errors associated to dispersion (Calamante et al., 2000), AIF was estimated close to the site of perfusion measurements. However, there is no reason to believe that AIF dispersion will be systematically different between MS patients and controls. To minimize the partial volume effects on AIF estimation (Axel, 1980), we used thin slices (3 mm).

Further studies are warranted to better explore the relationship between clinical and perfusion measures and to establish the role of the molecular mechanisms causing MS-related neurodegeneration. In particular, longitudinal studies in patients in the earliest stages of the disease will have to establish whether hemodynamic impairment is a mediator or a marker of degenerative tissue.

In summary, our findings suggest that DSC pMRI may reveal widespread microvascular NAWM abnormalities which are more marked in the PP-MS and may be clinically relevant. Although it remains speculative, DSC pMRI has the potential to provide a relevant objective measure of disease activity, and an MRI outcome measure to improve the evaluation of new therapies.

Acknowledgements

This work was supported by NIH grants R37 NS 29029-11, RO1 NS051623-01, and by Martin S. Davis Research Fellowship Endowment from the National Multiple Sclerosis Society.

References

Adams CW, Poston RN, Buk SJ, Sidhu YS, Vipond H. Inflammatory vasculitis in multiple sclerosis. J Neurol Sci 1985;69:269–283. [PubMed: 4031947]

Adams RA, Passino M, Sachs BD, Nuriel T, Akassoglou K. Fibrin mechanisms and functions in nervous system pathology. Mol Interv 2004;4:163–176. [PubMed: 15210870]

Axel L. Cerebral blood flow determination by rapid-sequence computed tomography: theoretical analysis. Radiology 1980;137:679–686. [PubMed: 7003648]

Bermel RA, Sharma J, Tjoa CW, Puli SR, Bakshi R. A semiautomated measure of whole-brain atrophy in multiple sclerosis. J Neurol Sci 2003;208:57–65. [PubMed: 12639726]

Brooks DJ, Leenders KL, Head G, et al. Studies on regional cerebral oxygen utilisation and cognitive function in multiple sclerosis. J Neurol Neurosurg Psychiatry 1984;47:1182–1191. [PubMed: 6334132]

Bruck W, Lucchinetti C, Lassmann H. The pathology of primary progressive multiple sclerosis. Mult Scler 2002;8:93–97. [PubMed: 11990878]

Calamante F, Gadian DG, Connelly A. Delay and dispersion effects in dynamic susceptibility contrast MRI: simulations using singular value decomposition. Magn Reson Med 2000;44:466–473. [PubMed: 10975900]

Carroll TJ, Rowley HA, Haughton VM. Automatic calculation of the arterial input function for cerebral perfusion imaging with MR imaging. Radiology 2003;227:593–600. [PubMed: 12663823]

Chang L, Ernst T, Leonido-Yee M, Speck O. Perfusion MRI detects rCBF abnormalities in early stages of HIV-cognitive motor complex. Neurology 2000;54:389–396. [PubMed: 10668700]

Evangelou N, Konz D, Esiri MM, et al. Regional axonal loss in the corpus callosum correlates with cerebral white matter lesion volume and distribution in multiple sclerosis. Brain 2000;123 (Pt 9): 1845–1849. [PubMed: 10960048]

Firbank MJ, Colloby SJ, Burn DJ, McKeith IG, O'Brien JT. Regional cerebral blood flow in Parkinson's disease with and without dementia. Neuroimage 2003;20:1309–1319. [PubMed: 14568499]

Haselhorst R, Kappos L, Bilecen D, et al. Dynamic susceptibility contrast MR imaging of plaque development in multiple sclerosis: application of an extended blood-brain barrier leakage correction. J Magn Reson Imaging 2000;11:495–505. [PubMed: 10813859]

Hauser, SL. Multiple sclerosis and other demyelinating diseases. In: Isselbacher, KJWJ.; Martin, JB.; Fauci, AS.; Kasper, DL., editors. Harrison's Principles of Internal Medicine. New York: McGraw-Hill; 1994. p. 2287-2295.

Ingle GT, Sastre-Garriga J, Miller DH, Thompson AJ. Is inflammation important in early PPMS? a longitudinal MRI study. J Neurol Neurosurg Psychiatry 2005;76:1255–1258. [PubMed: 16107362]

Johnson NA, Jahng GH, Weiner MW, et al. Pattern of cerebral hypoperfusion in Alzheimer disease and mild cognitive impairment measured with arterial spin-labeling MR imaging: initial experience. Radiology 2005;234:851–859. [PubMed: 15734937]

Kurtzke JF. Rating neurologic impairment in multiple sclerosis: an expanded disability status scale (EDSS). Neurology 1983;33:1444–1452. [PubMed: 6685237]

Lassmann H. Hypoxia-like tissue injury as a component of multiple sclerosis lesions. J Neurol Sci 2003;206:187–191. [PubMed: 12559509]

Latchaw RE. Cerebral perfusion imaging in acute stroke. J Vasc Interv Radiol 2004;15:S29–46. [PubMed: 15101514]

Law M, Saindane AM, Ge Y, et al. Microvascular abnormality in relapsing-remitting multiple sclerosis: perfusion MR imaging findings in normal-appearing white matter. Radiology 2004;231:645–652. [PubMed: 15163806]

Leary SM, Thompson AJ. Interferon beta-1a in primary progressive multiple sclerosis. J Neurol Sci 2003;206:215–216. [PubMed: 12559514]

Loevner LA, Grossman RI, Cohen JA, et al. Microscopic disease in normal-appearing white matter on conventional MR images in patients with multiple sclerosis: assessment with magnetization-transfer measurements. Radiology 1995;196:511–515. [PubMed: 7617869]

Lycke J, Wikkelso C, Bergh AC, Jacobsson L, Andersen O. Regional cerebral blood flow in multiple sclerosis measured by single photon emission tomography with technetium-99m hexamethylpropyleneamine oxime. Eur Neurol 1993;33:163–167. [PubMed: 8467826]

Manka C, Traber F, Gieseke J, Schild HH, Kuhl CK. Three-dimensional dynamic susceptibility-weighted perfusion MR imaging at 3.0 T: feasibility and contrast agent dose. Radiology 2005;234:869–877. [PubMed: 15665227]

McDonald WI, Compston A, Edan G, et al. Recommended diagnostic criteria for multiple sclerosis: guidelines from the International Panel on the diagnosis of multiple sclerosis. Ann Neurol 2001;50:121–127. [PubMed: 11456302]

Miller DH, Thompson AJ, Filippi M. Magnetic resonance studies of abnormalities in the normal appearing white matter and grey matter in multiple sclerosis. J Neurol 2003;250:1407–1419. [PubMed: 14673572]

Noseworthy JH. Progress in determining the causes and treatment of multiple sclerosis. Nature 1999;399:A40–47. [PubMed: 10392579]

Pozzilli C, Passafiume D, Bernardi S, et al. SPECT, MRI and cognitive functions in multiple sclerosis. J Neurol Neurosurg Psychiatry 1991;54:110–115. [PubMed: 2019835]

Putnam T. The pathogenesis of multiple sclerosis: a possible vascular factor. New England Journal of Medicine 1933;209:786–790.

Putnam T. Evidences of vascular occlusion in multiple sclerosis and encephalomyelitis. Arch Neurol Neuropsychol 1935;32:1298–1321.

Rashid W, Parkes LM, Ingle GT, et al. Abnormalities of cerebral perfusion in multiple sclerosis. J Neurol Neurosurg Psychiatry 2004;75:1288–1293. [PubMed: 15314117]

Rempp KA, Brix G, Wenz F, et al. Quantification of regional cerebral blood flow and volume with dynamic susceptibility contrast-enhanced MR imaging. Radiology 1994;193:637–641. [PubMed: 7972800]

Rosen BR, Belliveau JW, Buchbinder BR, et al. Contrast agents and cerebral hemodynamics. Magn Reson Med 1991;19:285–292. [PubMed: 1881317]

Rovaris M, Gallo A, Falini A, et al. Axonal injury and overall tissue loss are not related in primary progressive multiple sclerosis. Arch Neurol 2005a;62:898–902. [PubMed: 15956160]

Rovaris M, Gass A, Bammer R, et al. Diffusion MRI in multiple sclerosis. Neurology 2005b;65:1526–1532. [PubMed: 16301477]

Rudick RA. Disease-modifying drugs for relapsing-remitting multiple sclerosis and future directions for multiple sclerosis therapeutics. Arch Neurol 1999;56:1079–1084. [PubMed: 10488808]

Thompson AJ, Kermode AG, Wicks D, et al. Major differences in the dynamics of primary and secondary progressive multiple sclerosis. Ann Neurol 1991;29:53–62. [PubMed: 1996879]

Trapp BD, Peterson J, Ransohoff RM, et al. Axonal transection in the lesions of multiple sclerosis. N Engl J Med 1998;338:278–285. [PubMed: 9445407]

Trapp BD, Ransohoff R, Rudick R. Axonal pathology in multiple sclerosis: relationship to neurologic disability. Curr Opin Neurol 1999;12:295–302. [PubMed: 10499174]

Wakefield AJ, More LJ, Difford J, McLaughlin JE. Immunohistochemical study of vascular injury in acute multiple sclerosis. J Clin Pathol 1994;47:129–133. [PubMed: 8132826]

Warach S, Levin JM, Schomer DL, Holman BL, Edelman RR. Hyperperfusion of ictal seizure focus demonstrated by MR perfusion imaging. AJNR Am J Neuroradiol 1994;15:965–968. [PubMed: 8059669]

Wetzel SG, Cha S, Johnson G, et al. Relative cerebral blood volume measurements in intracranial mass lesions: interobserver and intraobserver reproducibility study. Radiology 2002;224:797–803. [PubMed: 12202717]

Wolinsky JS. The use of glatiramer acetate in the treatment of multiple sclerosis. Adv Neurol 2006;98:273–292. [PubMed: 16400839]

Wuerfel J, Bellmann-Strobl J, Brunecker P, et al. Changes in cerebral perfusion precede plaque formation in multiple sclerosis: a longitudinal perfusion MRI study. Brain 2004;127:111–119. [PubMed: 14570816]

Zettl UK, Kuhlmann T, Bruck W. Bcl-2 expressing T lymphocytes in multiple sclerosis lesions. Neuropathol Appl Neurobiol 1998;24:202–208. [PubMed: 9717185]

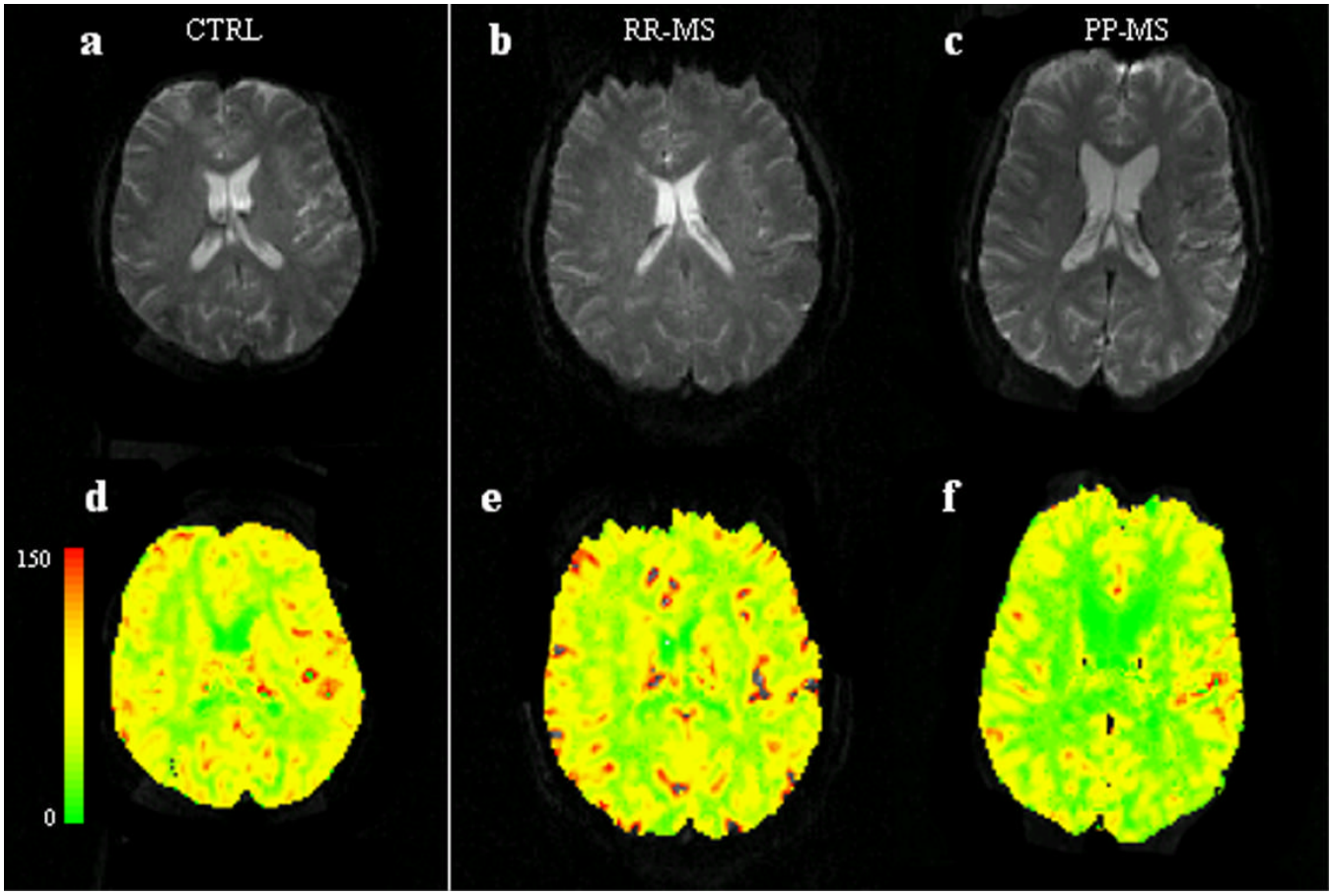

Fig. 1.

Top: Axial gradient-echo echo-planar MR image from a healthy control (**a**), a RR-MS patient (**b**) and a PP-MS patient (**c**).

Bottom: Axial gradient-echo echo-planar MR image from the same healthy control (**d**), a RR-MS patient (**e**) and a PP-MS patient (**f**) with CBF color-coded map overlay. The color bar indicates the CBF values (ml/100gr/min). Note generally lower CBF values on the color-coded map of the patient with PP-MS.

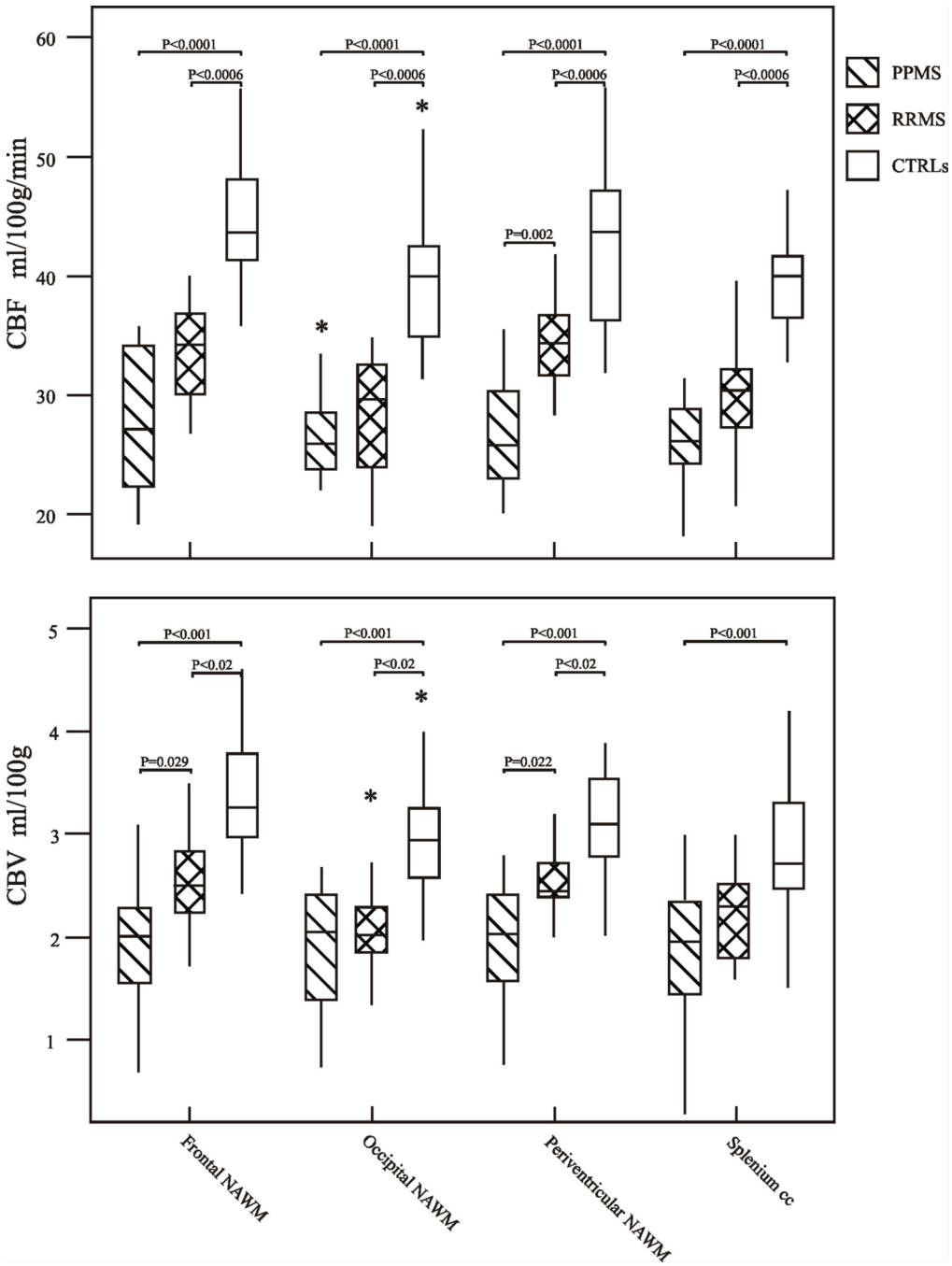

Fig. 2.

Top: Box plots display the 25%–75% values (boxes) ± 95% values (whiskers), median values (horizontal lines within boxes), and outliers (*) of absolute CBF value distribution in regions of frontal, periventricular, occipital NAWM and splenium of the corpus callosum among patients with PP-MS (hatched box), with RR-MS (crosshatched box) and in healthy controls (empty box).

Bottom: Box plots display the 25%–75% values (boxes) ± 95% values (whiskers), median values (horizontal lines within boxes), and outliers (*) of absolute CBV value distribution in regions of frontal, periventricular, occipital NAWM and splenium of the corpus callosum

between patients with PP-MS (hatched box), with RR-MS (crosshatched box) and in healthy controls (empty box). Only significant p values are reported.
Note that the median CBF and CBV values in PP-MS patients are lower than those in RR-MS patients, which in turn, are lower than those in controls.

Table 1

Demographic, Clinical and conventional MRI characteristics of 22 MS patients and of 11 healthy controls.

	PP-MS Patients (11)	RR-MS Patients (11)	Healthy Controls (11)
Mean Age, (range) y	53.63 (29–71)	46.18 (31–71)	50.82 (29–65)
Gender, F/M	4/7	8/3	7/4
Median EDSS Score, (range)	4.0 (3.0–7.0)	1.0 (0.0–6.5)	-
Median Disease Duration, (range) y	4.0 (1–19)	5.0 (1–13)	-
Mean T2 LV, mL (range)	7.33 (0.39–32.9)	5.20 (0.12–27.9)	-
Mean T1 LV, mL (range)	2.73 (0.04–21.5)	0.67 (0.04–3.20)	-

PP-MS = primary-progressive multiple sclerosis; RR-MS = relapsing-remitting multiple sclerosis; EDSS = Expanded Disability Status Scale; LV = lesion volume

Table 2

CBF, CBV and MTT values from four NAWM regions in PP-MS, RR-MS patients and healthy controls

	PP-MS Patients	RR-MS Patients	Healthy Controls
CBF (ml/100g/min)			
Periventricular NAWM	26.76±0.64	34.57±1.77	42.77±1.71
Frontal NAWM	27.67±1.24	33.68±1.84	44.87±0.85
Occipital NAWM	27.02±3.04	28.46±0.29	39.27±0.42
Splenium	25.98±1.84	31.14±1.98	40.16±1.98
CBV (ml/100g)			
Periventricular NAWM	1.93±0.12	2.54±0.13	3.23±0.59
Frontal NAWM	1.90±0.08	2.54±0.23	3.38±0.23
Occipital NAWM	1.92±0.15	2.06±0.17	2.94±0.18
Splenium	1.78±0.14	2.24±0.22	2.88±0.17
MTT (Seconds)			
Periventricular NAWM	4.30±0.24	4.43±0.20	4.38±0.90
Frontal NAWM	4.11±0.20	4.50±0.25	4.47±0.28
Occipital NAWM	4.11±0.23	4.31±0.20	4.49±0.16
Splenium	4.06±0.31	4.36±0.24	4.27±0.16

Values are given as means ± SD and adjusted for age and gender.

CBF = cerebral brain flow; CBV = cerebral brain volume; MTT = mean transit time; NAWM = normal-appearing white matter